Earth's Future

RESEARCH ARTICLE
10.1029/2021EF002394

The 2018–2020 Multi-Year Drought Sets a New Benchmark in Europe

Oldrich Rakovec[1,2], Luis Samaniego[1], Vittal Hari[1,3], Yannis Markonis[2], Vojtěch Moravec[2,4], Stephan Thober[1], Martin Hanel[2,4], and Rohini Kumar[1]

[1]UFZ-Helmholtz Centre for Environmental Research, Leipzig, Germany, [2]Faculty of Environmental Sciences, Czech University of Life Sciences Prague, Praha-Suchdol, Czech Republic, [3]Department of Environmental Science and Engineering, Indian Institute of Technology (ISM) Dhanbad, Dhanbad, India, [4]T. G. Masaryk Water Research Institute, Praha 6, Czech Republic

Key Points:

- The 2018–2020 multi-year drought shows unprecedented level of intensity during the past 250 years
- The 2018–2020 event reached record-breaking +2.8 K temperature anomaly and negatively impacted major crops
- Future drought events reach comparable intensity of 2018–2020 but with considerably longer durations

Supporting Information:

Supporting Information may be found in the online version of this article.

Correspondence to:

O. Rakovec, L. Samaniego, and R. Kumar,
oldrich.rakovec@ufz.de;
luis.samaniego@ufz.de;
rohini.kumar@ufz.de

Citation:

Rakovec, O., Samaniego, L., Hari, V., Markonis, Y., Moravec, V., Thober, S., et al. (2022). The 2018–2020 multi-year drought sets a new benchmark in Europe. *Earth's Future*, *10*, e2021EF002394. https://doi.org/10.1029/2021EF002394

Received 25 AUG 2021
Accepted 11 MAR 2022

Abstract During the period 2018–2020, Europe experienced a series of hot and dry weather conditions with significant socioeconomic and environmental consequences. Yet, the extremity of these multi-year dry conditions is not recognized. Here, we provide a comprehensive spatio-temporal assessment of the drought hazard over Europe by benchmarking past exceptional events during the period from 1766 to 2020. We identified the 2018–2020 drought event as a new benchmark having an unprecedented intensity that persisted for more than 2 years, exhibiting a mean areal coverage of 35.6% and an average duration of 12.2 months. What makes this event truly exceptional compared with past events is its near-surface air temperature anomaly reaching +2.8 K, which constitutes a further evidence that the ongoing global warming is exacerbating present drought events. Furthermore, future events based on climate model simulations Coupled Model Intercomparison Project v5 suggest that Europe should be prepared for events of comparable intensity as the 2018–2020 event but with durations longer than any of those experienced in the last 250 years. Our study thus emphasizes the urgent need for adaption and mitigation strategies to cope with such multi-year drought events across Europe.

Plain Language Summary This manuscript demonstrates that the 2018–2020 multi-year drought event constitutes a new benchmark in Europe, with an unprecedented level of intensity over the past 250 years. What makes this event truly exceptional compared with past events is its temperature anomaly reaching +2.8 K. This finding provides new evidence that the ongoing global warming exacerbates current drought events. The key message of this study is that the projected future events across the European continent will have a comparable intensity as the 2018–2020 drought but exhibit considerably longer durations than any of those observed during the last 250 years. Our analysis also shows that these exceptional temperature-enhanced droughts significantly negatively impact commodity crops across Europe.

1. Introduction

The observed increase in the frequency of droughts and heatwaves over the Northern Hemisphere in the 21st century poses immediate socio-economic threats affecting the well-being of the people by triggering negative health effects. These adverse hydro-meteorological conditions can lead to agricultural and ecological impacts such as crop losses, poor water quality conditions in water bodies, and wildfires. The reduction of the streamflow resulting from a drought event combined with high air temperatures also creates a threat to existing infrastructure. Several authors have reported cases of reduction of the cooling capacity in power plants, the reduction of tonnage in fluvial transportation, and the drop in reservoir storage leading to drinking water shortages (Naumann et al., 2021; Peichl et al., 2018; Stanke et al., 2013; Vogel et al., 2019). Europe, in particular, has experienced a series of dry summers with substantial socioeconomic and environmental impacts in 2003 (Fischer et al., 2007), 2010 (Flach et al., 2018), 2015 (Van Lanen et al., 2016) and 2018–2020 (Hari et al., 2020; Peters et al., 2020). The latest report of the European Commission estimates that the current annual monetary losses across Europe due to droughts were 9 billion EUR every year. Depending on the region, between 39% and 60% of the losses are related to agriculture, 22%–48% to the energy sector, while 9%–20% of the total damages correspond to public water supply systems (Naumann et al., 2021). Besides direct financial losses, the natural net ecosystem carbon uptake can get further significantly reduced by drought conditions (Ciais et al., 2005).

The reconstructions of hydro-climatic data suggest that the recent sequence of European summer droughts is unprecedented during the past centuries (Büntgen et al., 2021)—with reported several multi-year droughts (2018–2019 [Hari et al., 2020] and 2014–2018 [Moravec et al., 2021]). While the characteristics and impacts of individual drought years are well described in the literature (Moravec et al., 2019; Peters et al., 2020; Van Lanen et al., 2016), the simultaneous evolution of droughts in space and time is rarely explored (Herrera-Estrada et al., 2017). Furthermore, the severity of the recent droughts highlights the concern that global warming may be significantly contributing to their evolution (Williams et al., 2020) and that its effects will continue to exacerbate them in the future (Hari et al., 2020; Samaniego et al., 2018). A comprehensive long-span benchmarking of droughts, considering their space-time evolution, is therefore urgently needed to be able to place the recent multi-year drought within the variability in the observational period and the near and long-term projections. By doing so, we substantiate how exceptional this recent drought event is in the historical record and the likelihood of such events under different future climate scenarios.

In this study, we benchmark the recent droughts from a long-term perspective taking into account the spatio-temporal evolution of drought propagation across Europe. Our drought analysis is based on characterizing anomalous conditions of root-zone soil moisture that reflect the antecedent and contemporary hydro-meteorologic conditions and constitutes the primary source of water for plant growth (Andreadis et al., 2005; Seneviratne et al., 2010). The soil moisture is estimated with the well-established mesoscale Hydrologic Model (mHM) (Kumar et al., 2013; Samaniego et al., 2010) (Section 2.3). The monthly soil moisture estimates are transformed into a percentile-based monthly soil moisture index (SMI (Samaniego et al., 2013))—which is then taken as a basis for clustering the space-time evolution of soil moisture droughts (Samaniego et al., 2013, 2018). Finally, we quantify the drought characteristics (i.e., areal extent, duration, total drought magnitude, and intensity, see Section 2.4) from 1766 to 2100; the period 1766–2020 corresponds to observation-based simulation (reference), and further, we quantify these characteristics in the climate models and also analyze the changes of these under moderate and high emission scenarios (1950–2100; see Section 2.1).

2. Data and Methods

2.1. Meteorological Model Forcing Data

2.1.1. Observation-Based Historical Forcing Data

This study is mainly based on the precipitation and near-surface air temperature observation-based data sets for the period 1766–2015 (Casty et al., 2007) and E-OBS v21 (Hofstra et al., 2009) (daily gridded observational data set for precipitation, and temperature in Europe) available for the period 1950–2020. The overlapping period allowed for correction of biases (Gudmundsson et al., 2012) in the data set of Casty with respect to E-OBS (Hanel et al., 2018; Moravec et al., 2021), and the merged meteorologic product is used as an input into the mHM (Kumar et al., 2013; Samaniego et al., 2010) to obtain the soil moisture simulations. The estimates of potential evapotranspiration required by mHM are based on mean near-surface air temperature and approximations for extraterrestrial solar radiation (Oudin et al., 2005) during the historical period.

2.1.2. Climate Model Forcing Data

Besides the observation-based model forcings, we utilized the bias corrected daily precipitation, average, maximum and minimum temperature fields at 0.5° resolution were made available by the ISI-MIP project (Warszawski et al., 2014). This suite is based on five Coupled Model Intercomparison Project v5 (CMIP5) Global Climate Models (HadGEM2-ES, IPSL-CM5A-LR, MIROC-ESM-CHEM, GFDL-ESM2M and NorESM1-M) in the historical mode and under two future representative concentration pathways (RCP4.5 and RCP8.5). The trend-preserving bias correction method (Hempel et al., 2013) was used in the ISI-MIP project to match the climatology of the CMIP5 GCMs with observations. We refer to Frieler et al. (2017) and Warszawski et al. (2014) for a full description of the ISIMIP experiment, as detailed descriptions of the climate model projection used in this study are beyond the scope of the present study. The five models selected for the ISI-MIP project follow the strategy to represent warm and wet and cold and dry climates, which are most relevant for impact studies (Frieler et al., 2017). Each of the GCMs is available at a single realization. Thus internal climate variability and uncertainty due to initial conditions are not considered in the ISIMIP-2b experiment. The Penman-Monteith potential evapotranspiration method (Allen et al., 1998) also needed as forcing for mHM is based on the surface energy budget (i.e., Rn-G = SH + LH), where Rn, G, SH, and LH are the net radiation, ground heat flux, and sensible

and latent heat flux (Scheff & Frierson, 2014), respectively. This approach implicitly considers the ambient CO_2 effects on plant transpiration, vegetation growth (Trnka et al., 2019).

2.2. Crop Yield Data

We utilized the data of agriculture yields 1961–2019 from Food and Agriculture Organization of the United Nations (FAO Global Statistical Yearbook, 2021) and harvested production and areas under cultivation 2010–2020 from EUROSTAT (2021). The overlapping period 2010–2019 was used for data quality checks between both data sets and supplementing missing data. We considered three dominant kinds of cereals: wheat, grain maize and barley as representative set of agricultural production. To account for technological advances (e.g., improvements in plant genetics, fertilizer, pesticides) (Lu et al., 2017) the systematic linear trend was removed from data of agriculture yields of given crops. Three-year rolling mean was then applied on these detrended data to smooth out the year-to-year variability. Finally, the percentage difference of 3 year rolling mean from the base linear trend was calculated to express crop yield deviation of a given 3 year period for each country.

2.3. Mesoscale Hydrologic Model

The mHM (Kumar et al., 2013; Samaniego et al., 2010) is a spatially explicit, grid-based hydrologic model developed at the UFZ-Helmholtz Centre for Environmental Research (Samaniego, Kaluza, et al., 2019) aiming at providing seamless prediction of hydrological fluxes and storages at multiple spatial resolutions and locations across the globe and it has reached Technology readiness levels of 9. The model uses the grid cell as a primary hydrologic unit, and accounts for the following hydrological processes: canopy interception, snow accumulation and melt, soil moisture and evapotranspiration, surface and subsurface runoff generations, deep percolation and baseflow, and flood routing along with a river network. mHM uses a novel Multiscale Parameterization Regionalization technique which includes the regionalization and spatial scaling approaches to generate a set of regionalized model parameter fields at required modeling resolutions, while explicitly accounting for the sub-grid variability of the fine-scale information on terrain, soil, vegetation, and other landscape properties (Samaniego et al., 2017).

The calibration of the mHM parameters was conducted and demonstrated earlier (Samaniego, Thober, et al., 2019), and was based on the multi-basin optimizations performed on a wide range of hydrologic regimes. The 48 transfer function parameters used in mHM were estimated simultaneously at nine ($N = 9$) geographically and hydro-climatically diverse basins across the European domain. This procedure was repeated 30 times. Thus, 30 different parameter sets were obtained tailor-made to different groups of nine "donor" basins. Each optimization run was carried out with the Dynamically Dimensioned Search algorithm (Tolson & Shoemaker, 2007) using 1,500 iterations. The Kling-Gupta Efficiency (KGE) (Gupta et al., 2009) obtained between simulated and observed daily streamflow for each selected basin was used as an objective function. Each of the 30 optimized parameter sets was then cross-validated in 1,266 European river basins having at least 5 years of streamflow records. The parameter set that exhibited the best performance using the median daily KGE in the cross-validation test was used for the final runs (KGE = 0.55) for obtaining seamless soil moisture predictions across Europe and is depicted by a black line in Figure S1 in Supporting Information S1.

2.4. Drought Analysis

Understanding of continental-wide drought propagation and its changes over time require methods which quantify drought areal extent and duration together with drought severity in a combined manner. The spatio-temporal drought cluster analysis (Andreadis et al., 2005; Diaz et al., 2020; Lloyd-Hughes, 2012; Samaniego et al., 2013; Zhou et al., 2019; Zink et al., 2016) allow to track events in space and time and thus to quantify their characteristics across domain and over the entire period. To quantify agricultural droughts we use the deficit of the mHM simulated soil moisture with respect to its seasonal climatology at a given grid cell. The index is called (SMI) (Sheffield et al., 2004) and its implementation has been described in the past (Samaniego et al., 2013) as follows. The SMI varies between two limits 0 and 1. The lower bound indicates the driest condition with respect to the reference period, whereas the upper bound indicates the wettest. The $SMI_{i,m}$ is estimated such that it represents the conditional cumulative distribution function of the soil water content in the root zone at a given grid cell i at the calendar month m. Given a time series $x_1, x_2, \ldots, x_n$ that corresponds to the soil moisture fractions of a

given cell at calendar month m (e.g., January), the kernel density estimate at a given value x can be obtained by $\hat{f}(x) = \frac{1}{nh}\sum_{k=1}^{n} K\left(\frac{x-x_k}{h}\right)$, with $K(x)$ denoting a Gaussian smoothing kernel, n the sampling size, and h the bandwidth. The SMI for a soil moisture fraction value x is estimated with the quantile function by numerically integrating the following expression $\mathrm{SMI} = \int_0^x \hat{f}(u)du$.

To estimate spatio-temporal drought clusters we follow this procedure (Samaniego et al., 2013). First, we select regions under drought by masking the SMI fields: $\mathrm{SMI}_t < \tau$, with $\tau = 0.2$, according to Andreadis et al. (2005) and Vidal et al. (2010). Second, consolidate spatial drought clusters at every time step. Clusters with an area of less than $\eta \times A_c$ are neglected, with A_c the area of a grid cell. In this study $\eta \approx 10$ and $\eta \times A_c > 25{,}000\ \mathrm{km}^2$ was selected. This subjective choice is necessary to eliminate small isolated areas that are suffering a drought but are too small to be considered as a regional event, and it does not have an impact on large-scale cluster characteristics. On the final step, independent spatial drought clusters over successive time steps are consolidated into regional, multi-temporal clusters. The only condition to join spatial clusters over consecutive time steps is that their overlapping area is larger than $\iota \times A_c$, with $\iota \approx 60$. It represents the connectivity between the clusters of two consecutive time periods. Events having an intersection area at any sequential time step of less than this threshold are considered independent events. The SMI code that executes this algorithm is available at https://git.ufz.de/chs/progs/SMI (Samaniego et al., 2022). The drought severity (S_d) for a grid cell over a duration d (in months) is estimated by integrating the masked SMI fields over time: $S_d = 1 - \frac{1}{d}\sum_{t\in d} \mathrm{SMI}_t$. This indicator aims to measure the duration and intensity of drought event. It ranges from zero to one, with one denoting locations with the strongest impact during interval d. The total magnitude of a drought event is defined as the spatio-temporal integral of the SMI under the deficit threshold τ, explicitly: $M = \sum_{t=t_0}^{t_1} \int_{A_t} (\tau - \mathrm{SMI}_i(t))_+ \, dA$. Here, t_0 and t_1 denote the onset and the ending months of a drought event. A_t is the area under drought at time point t expressed as the percentage of total drain area (in this case Europe); and $(\cdot)_+$ is the positive part function. Hence, M is expressed in [months × %Total Area]. The intensity of a drought event (I_d) is obtained by normalizing M by the arbitrary drought duration d [months] from the onset: $I_d = \frac{1}{d}\sum_{t=t_0}^{t_0+d} \int_{A_t} (\tau - \mathrm{SMI}_i(t))_+ \, dA$ expressed in [%Total Area]. Note that drought intensity changes over time from the drought onset, while the drought magnitude is here estimated for the entire cluster.

The values of M and I_d are accompanied by "mean drought characteristics" of an identified drought cluster/event in terms of "mean drought area over time" as a fraction of European domain [in %] and "mean duration over space" of identified drought cluster [in months]. Here, consider that a drought cluster dynamically evolves over space and time. First, it gets initiated, then it evolves/increases, and finally, it gets terminated. For example, the drought cluster/event of 2018–2020 was initiated in April 2018 and lasted until December 2020. Although it took 33 months from t_0 to t_1, its "mean duration," averaged over entire cluster domain, yields 12.2 months.

Historical and future extreme soil moisture drought events are estimated by forcing mHM with the respective meteorological outputs of the GCMs (Section 2.1.2). To maintain the consistency with the historical drought analysis, the GCM specific soil moisture distribution functions estimated during the period from 1950 to 2020 were taken as a reference for estimating the soil moisture droughts in future. The drought characteristics are calculated for each model realization separately, to avoid a smoothing effect of averaging, in other words, to be able to generate extremes (rare events) realistically.

3. Results and Discussion

The spatio-temporal analysis of the largest European soil moisture droughts since 1766, summarized in Figure 1a, reveals three outstanding and well-comparable soil moisture drought events in terms of areal coverage, duration from the onset, and drought intensity: 1857–1860, 1920–1922, and 2018–2020. The 2018–2020 event exhibits the largest mean drought area over time, covering approximately on average 36% of Europe with a mean duration over space of 12.2 months. Note that these characteristics reflect the average behavior accounting for the spatio-temporal development of the drought events (see Section 2.4). Concerning duration, the 2018–2020 event ranks second after the event of 1857–1860. Additionally, we highlight other four well-documented and significant European drought events (Masante et al., 2019): 1947–1948, 1975–1977, 2003–2004, and 2015–2016. Figure S2 in Supporting Information S1 shows the negligible effect of the varying cluster parameter ι on the soil moisture cluster identification. The 2018–2020 drought event is identified as the largest across a range of $\iota = 40$,

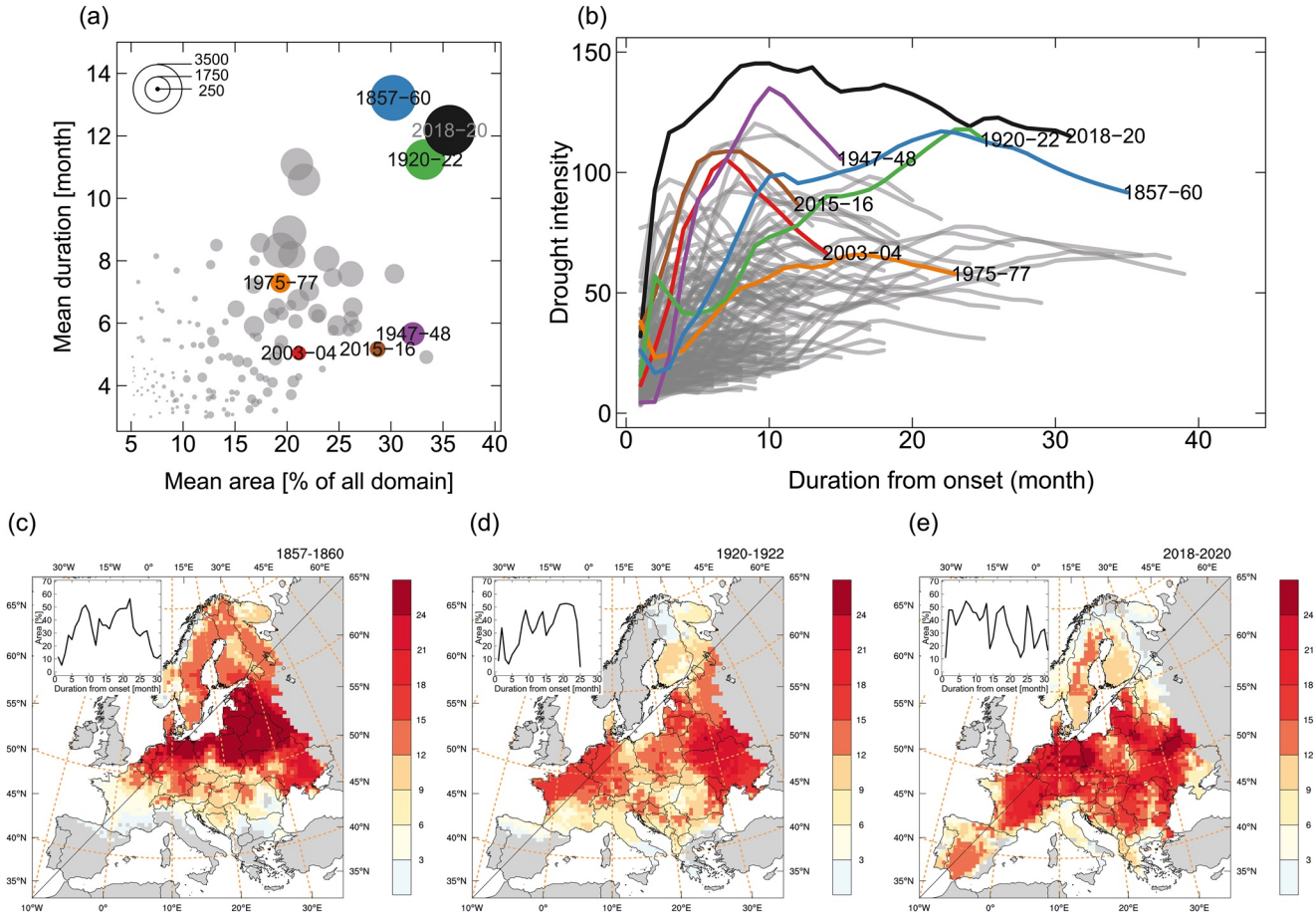

Figure 1. Main characteristics of the three largest soil moisture drought clusters identified in Europe since 1766. (a) Scatter plot of the mean area and duration of European droughts from 1766 to 2020 based on the mesoscale Hydrologic Model simulations forced with reconstructed and observation-based historical forcing data. The cluster labels define period (start year–end year) of the well-known drought events. The bubble size corresponds to the total drought magnitude [-] (b) Temporal evolution of the drought intensity from the onset of the drought. The 2018–2020 event exhibits the largest drought intensity in comparison to all other events overall time (c–e) Spatial map depicting the mean drought duration [months] of the 1857–1860, 1920–1922, and 2018–2020 events. The inset plot shows the temporal evolution of the areal coverage from the onset of the corresponding event.

50, 60, 70, 80 values, which yield areal coverage range between 35.1% and 36.5% and average duration range of 12.0–12.5 months.

In this context, what makes the 2018–2020 event outstanding with respect to the other events is the strong temporal development of its mean intensity since the onset of the drought event (Figure 1b). We refer to intensity as the total drought magnitude normalized by its duration (see Section 2.4). The 2018–2020 event has the steepest and continuous rise in intensity reaching a historical maximum after only 10 months from the onset, while reaching 80% of their maximum intensity within 4 months only. Furthermore, we notice that the four exceptional summer droughts with the steepest rise in intensity (1947–1948, 2015–2016, 2003–2004, 2015–2016, and 2018–2020) have been always initiated in spring (April–May) primarily as a result of compound effects of low precipitation and high air temperatures leading to severe soil water deficits (Ionita et al., 2020). After the highest intensity is reached, it usually takes between 6 and 12 months until a drought event terminates (Figure 1b). This point is reached in most cases during the following winter and spring seasons due to the significant contribution of the snowmelt. For example, the 2003 and 2015 warm-season events, which quickly built their peak intensity during late spring and summer, and slowly vanished in the following year leading to a recovery of the vegetation health status (Hari et al., 2020). There has been generally a continuous rise in the intensity and its peak since the beginning of the 21st century (Figure 1b, progression in peak intensity from 2003 to 2004, 2015–2016, 2018–2020).

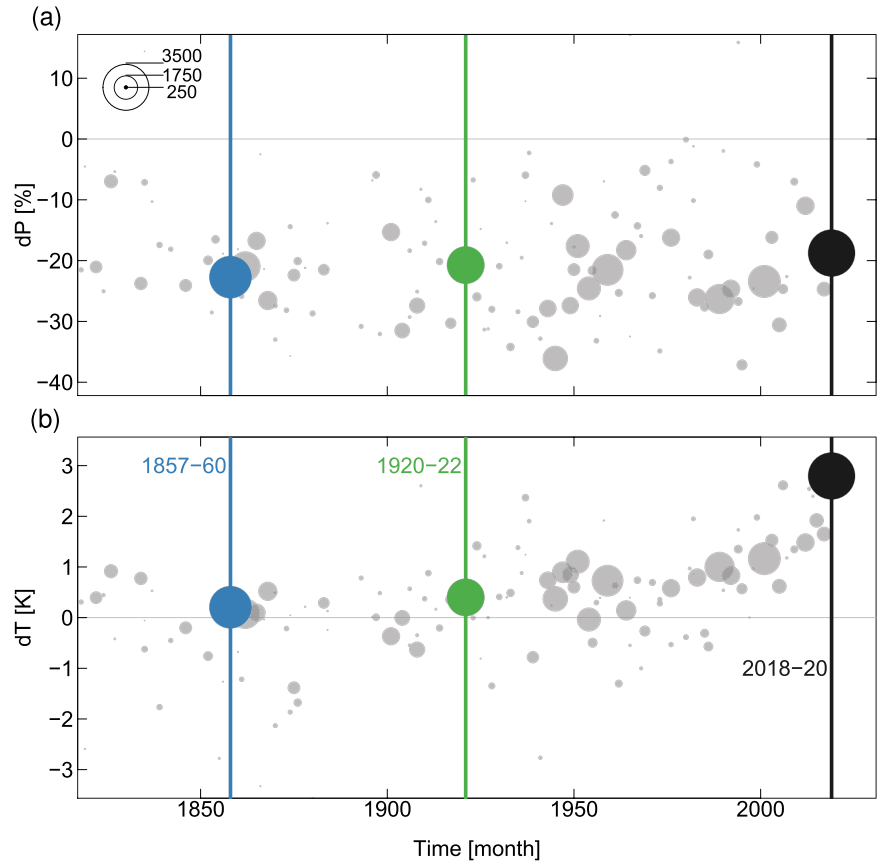

Figure 2. Meteorological conditions during the soil moisture droughts from 1766 to the present. Average relative precipitation anomaly and average absolute near-surface air temperature anomaly based on the monthly climatology during the period 1766–2020. The bubble size corresponds to the total drought magnitude. The colored bubbles correspond to the three major events depicted in Figure 1a.

The spatial distribution of the mean drought duration for the three largest events (Figures 1c–1e) suggest that the 2018–2020 event "extended" across entire Europe, which has so-far never happened for any other major events in the past. Our simulations reveal that 20% (40%) of the European domain was under drought for more than 18 (12) months during 2018–2020. The inset of Figure 1e depicts the temporal evolution of the area under drought, which exhibits a lot of variability reaching a maximum of 50% of Europe's area was affected by a drought. The 2018–2020 event, exhibited several peaks in the evolution of drought coverage (snapshots of four states are provided in Figure S3 in Supporting Information S1: The centroid of this drought event is located in the central and eastern Europe, although during 2018 the event covered parts of Scandinavia). In 2019, it expanded to the Mediterranean region, which corresponds well with the entry of the European Drought Observatory database (Masante et al., 2019).

Büntgen et al. (2021) showed that the recent sequences of European seasonal droughts are unprecedented at a millennial time scale, suggesting that amplification in anthropogenic warming may have played a significant role in exacerbating its evolution. To analyze the role of near-surface air temperature and precipitation conditions on the soil moisture droughts, we quantify the mean precipitation and temperature anomalies over the area affected by corresponding drought events, as depicted in Figure 2. It reveals that the precipitation deficit during the 2018–2020 event is around 20% with respect to the long term mean and therefore comparable to previous major drought events. This event, however, is exceptional considering the record-breaking high-temperature anomaly that reached up to +2.8 K with respect to the long term mean. This finding indicates the amplifying effect of temperature on drought evolution as depicted by Chiang et al. (2018). We also noticed a rather localized event over the Mediterranean region, where precipitation deficit is one of the largest in relative terms (up to 35%), but that did not induce considerable changes in the soil moisture deficit with a large areal coverage and/or multi-year

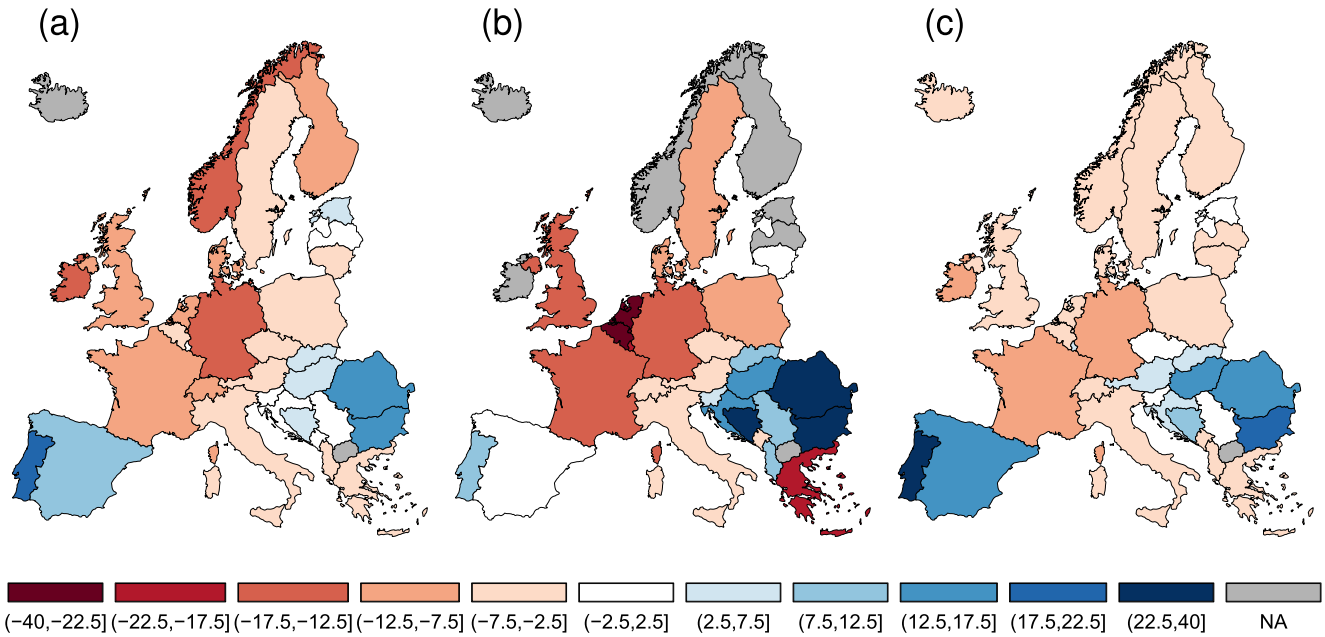

Figure 3. Crop yield anomaly. Average percent crop yield anomaly during 2018–2020 with respect to 1961–2021 period (after removal of linear trend representing technological advances) for three major cereals: (a) wheat, (b) grain maize, and (c) barley during period 1961–2021 (EUROSTAT, 2021; FAO Global Statistical Yearbook, 2021).

duration. Additionally, the corresponding temperature anomaly was close to zero. These investigations were focused on providing a glimpse on the anomalous meteorological conditions associated with large-scale soil moisture drought events occurred across Europe. However, a proper attribution of disentangling the explicit control of different drivers including meteorological and other (land-surface feedback) conditions (Seneviratne et al., 2010) require careful considerations, which is beyond the scope of current work.

The aforementioned analysis establishes the 2018–2020 drought as a record breaking event over the past 250 years. Considering the high impacts of events like 2018–2020, the dominant role of the rain-fed agriculture in Europe (Trnka et al., 2019), and the negligible mitigation effect of irrigation systems on drought stress at continental scales (especially in Central Europe), next we scrutinize how soil moisture droughts have affected cropland in Europe during the last seven decades, during which consistent crop yield data are available (EUROSTAT, 2021; FAO Global Statistical Yearbook, 2021). We analyze the possible impact of soil moisture drought on the loss in agriculture productivity across Europe. Figure 3 shows a substantial drop in major crop yields (wheat, grain maize, and barley) during the 2018–2020 drought event across most of the European countries. The 3-year average crop yield anomaly for three dominant cereals is considered after removing the systematic linear trend accounting for technological advances (e.g., improvements in plant genetics, fertilizer, pesticides). All three cereal products exhibit sharp decline from the expected (linear trend) yields across western, central and northern Europe: losses of up to 17.5% for wheat in Germany, 20%–40% for grain maize in western Europe (including Benelux, Germany, and France) and around 10% losses for barley in most countries in Europe except for the Iberian Peninsula and several south-eastern European countries. The extremity of the expected crop yield losses is further depicted in Figure S4 in Supporting Information S1, which shows the 3 year exceedance probability of the averaged ranks (Benard & Bos-Levenbach, 1953).

Considering the extremity of the 2018–2020 event, it is imperative to understand how the characteristics of this event compare with those of future alike events. To this end, we compare the areal extent, the duration, and the total drought magnitude of this 2018–2020 event against those of potential events resulting from climate projections. Figures 4a and 4b shows that the 2018–2020 event ranks as one of the most extreme when compared against GCM simulated events during the 1950–2020 period, in terms of both areal coverage and duration. It is worth noting that Figures 4a and 4b integrates all three drought aspects: severity, duration and area from all five GCMs at once. Ensemble averaging in this case due to the fact that under different climate forcing's data, droughts evolve during different times; they do not happen at the exact location.

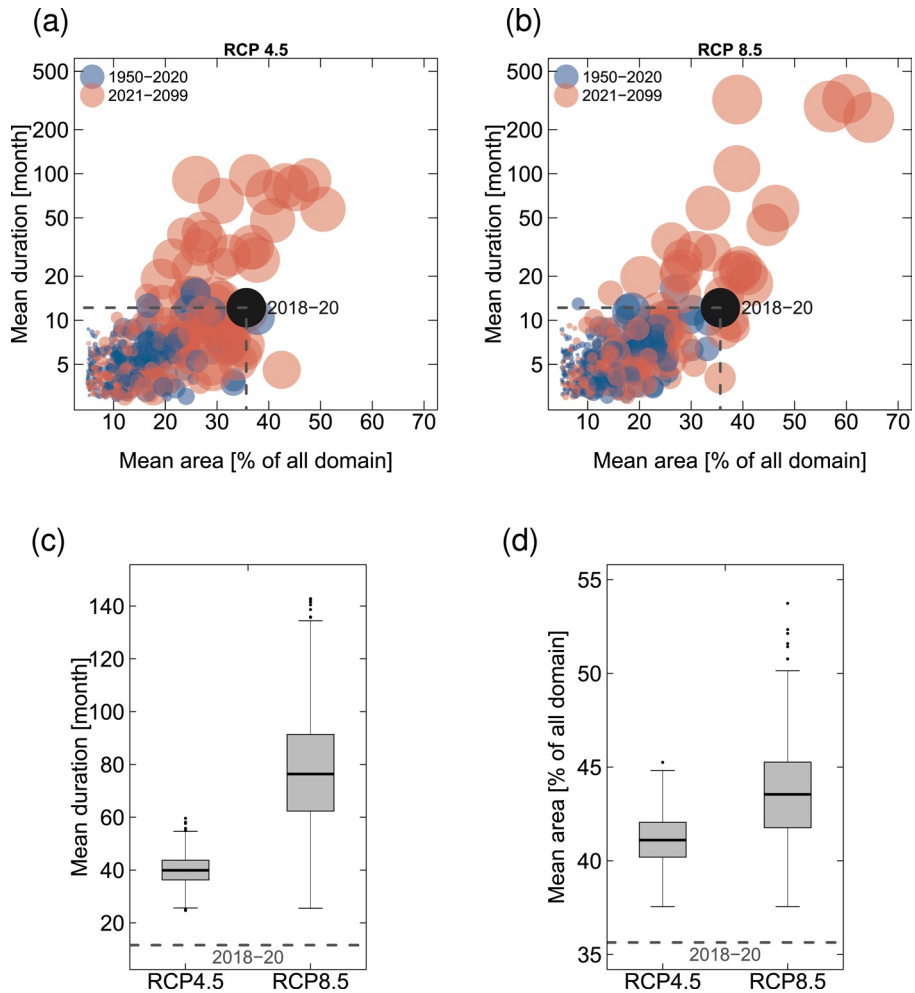

Figure 4. Main characteristics of large soil moisture drought events based on five Global Climate Models (GCMs). Bubble plot depicting areal extent, duration and normalized magnitude (intensity) of the drought events in Europe during the 1950–2020 and 2021–2099 periods, based on the (a) representative concentration pathways (RCP 4.5) and (b) RCP 8.5, respectively. The drought intensity is proportional to the circle size. The benchmarking 2018–2020 drought event, derived from observation-based simulations from Figure 1, is included for comparison. The boundary drawn by the dashed gray lines denotes events whose areal extent or duration are greater than the 2018–2020 event. The sampling distributions of the mean duration and mean areal drought extent across five GCMs corresponding to the RCPs 4.5 and 8.5 during 2021–2099, for events larger than the benchmark historical 2018–2020 event, are depicted in panels (c) and (d), respectively.

The spatio-temporal evolution of future soil moisture droughts during the period from 2021 to 2099 suggests that the most extreme droughts are projected to be significantly longer (RCP4.5: up to 100 months; RCP8.5: up to 300 months) than that of the 2018–2020 drought event. This result is in line with the previous study (Samaniego et al., 2018), and the longer duration of RCP8.5 is projected independently by all five GCMs (see Figure S5 in Supporting Information S1). While the moderate RCP4.5 emission scenario projects the most significant drought clusters to cover up to 50% of the entire domain, this areal extent reaches up to 65% based on the high-emission scenarios. Additionally, the 2018–2020 event dominates all GCM-based events in terms of drought intensity during the historical period, similar to what was seen with the observation-based events (see Figure S6 in Supporting Information S1). Only a few future RCP's realizations show greater intensity than that of the 2018–2020 event. Here, the climatological conditions defining the soil anomalies are based on the contemporary conditions (1950–2020), assuming there is no adaption to persistent drying patterns considered. This allows the drought to develop for a longer duration to develop into a multiple-year drought. Our analysis cannot confirm higher occurrence frequencies for a 2018–2020-like event in the future. The reason for that is that our GCM

simulations are limited until 2100. However, a future event can evolve for a long time given the drought threshold set in our analysis.

Figures 4c and 4d depicts two individual drought characteristics in terms of the sampling distribution of the mean duration and the mean areal extent of the GCM-derived drought events under both RCPs to illustrate their differences in projected future drought characteristics of all events greater than historical 2018–2020 benchmark. On average, future drought events whose duration is greater than the 2018–2020 event are projected to last approximately 40 months (range: 25–60 months) under the moderate emission scenario, while they will nearly double their duration (range: 25–180 months) under a high-emission scenario (Figure 4c). This implies that future events could last, on average, three to six times longer than the 2018–2020 event, respectively. With respect to the areal extent, we observe a slight increase from 41% to 43% (Figure 4d), between RCP 4.5 and 8.5, which corresponds to an increase of 14%–20% with respect to the 2018–2020 event, respectively.

4. Summary and Conclusions

We synthesized long-term simulations showing the spatio-temporal evolution of soil moisture droughts in Europe during the period from 1766 to 2020. Our analysis helped to better understand the development of multi-year droughts by taking into account long-term historical changes in hydroclimatic variability. We concluded that the recent 2018–2020 drought event is exceptional because of its significantly higher intensity and fast development from its onset compared to past events. Our study highlights that the 2018–2020 drought event, compared to all historical events, emerges as a new benchmark that can be used to gauge the potential impact of future drought events in terms of socioeconomic and ecological damages in Europe. From our recent analysis, and in accordance with previous study (Samaniego et al., 2018), we conclude that Europe should prepare adaptation and mitigation plans for future events whose intensity may be comparable to the previous event, but whose duration (and partly their spatial extent) will be much greater than any event observed in the last 250 years. Our analysis shows that exceptional agricultural droughts enhanced by record-breaking near-surface air temperature anomalies have significant impact (decline) on crop yields across the European countries. Soil moisture drought projections synthesized in this study, even under a moderate emission scenario, indicate that decision-makers in Europe should be prepared for drought events of comparable intensity in future. Thus, the 2018–2020 drought event could be considered as a wake-up call on agricultural policies. In this study, we compared and contrasted this event with earlier events of similar magnitudes and showed the role of increasing temperature rises. This study has focused on detecting the soil moisture droughts and their driving meteorological conditions. Future studies should aim at disentangling the roles of precipitation and temperature drivers, including climate model runs. Finally, we emphasize the need for new technological developments to mitigate the effects of extreme droughts and heatwaves and further research to understand how this new kind of fast intensified droughts will impact human health, ecosystems, and, ultimately, our living conditions.

Data Availability Statement

Data analysis was conducted at the High-Performance Computing (HPC) Cluster EVE, a joint effort of both the Helmholtz Centre for Environmental Research-UFZ and the German Centre for Integrative Biodiversity Research (iDiv) Halle-Jena-Leipzig. Model simulations used in this study can be obtained from https://dx.doi.org/10.5281/zenodo.5082089. The mHM (v5.10) code can be found at Samaniego, Kaluza, et al. (2019) and the SMI code can be found under Samaniego et al. (2022). OR and RK conceptualized and designed the study with inputs from LS. OR conducted the hydrologic simulations and analysis with inputs from LS, VH, YM, MH, and RK. LS and ST provided the SMI code. VM processed the crop yield data. OR wrote the initial draft with inputs from LS, VH and RK. All authors contributed to discussion and edited the manuscript.

Acknowledgments
This work was carried out within the bilateral project eXtreme EuRopean drOughtS (multimodel synthesis of past, present and future events), funded by the Deutsche Forschungsgemeinschaft (grant RA 3235/1-1) and Czech Science Foundation (grant 19-24089J). The authors would also like to thank the partial funding from the Helmholtz Climate Initiative project. We acknowledge Song Feng (the University of Nebraska–Lincoln) for sharing and processing potential evapotranspiration from the Coupled Model Intercomparison Project v5 archive. Open access funding enabled and organized by Projekt DEAL.

References

Allen, R. G., Pereira, L. S., Raes, D., & Smith, M. (1998). Crop evapotranspiration-Guidelines for computing crop water requirements-FAO Irrigation and drainage paper 56. *Fao, Rome*, *300*(9), D05109.

Andreadis, K. M., Clark, E. A., Wood, A. W., Hamlet, A. F., & Lettenmaier, D. P. (2005). Twentieth-century drought in the conterminous United States. *Journal of Hydrometeorology*, *6*(6), 985–1001. https://doi.org/10.1175/jhm450.1

Benard, A., & Bos-Levenbach, E. (1953). The plotting of observations on probability paper. *Statistica*, *7*, 163–173. https://doi.org/10.1111/j.1467-9574.1953.tb00821.x

Büntgen, U., Urban, O., Krusic, P. J., Rybníček, M., Kolář, T., Kyncl, T., et al. (2021). Recent European drought extremes beyond Common Era background variability. *Nature Geoscience*, *14*(4), 190–196. https://doi.org/10.1038/s41561-021-00698-0

Casty, C., Raible, C. C., Stocker, T. F., Wanner, H., & Luterbacher, J. (2007). A European pattern climatology 1766–2000. *Climate Dynamics*, *29*(7–8), 791–805. https://doi.org/10.1007/s00382-007-0257-6

Chiang, F., Mazdiyasni, O., & AghaKouchak, A. (2018). Amplified warming of droughts in southern United States in observations and model simulations. *Science Advances*, *4*(8), eaat2380. https://doi.org/10.1126/sciadv.aat2380

Ciais, P., Reichstein, M., Viovy, N., Granier, A., Ogée, J., Allard, V., et al. (2005). Europe-wide reduction in primary productivity caused by the heat and drought in 2003. *Nature*, *437*(7058), 529–533. https://doi.org/10.1038/nature03972

Diaz, V., Perez, G. A. C., Van Lanen, H. A. J., Solomatine, D., & Varouchakis, E. A. (2020). An approach to characterise spatio-temporal drought dynamics. *Advances in Water Resources*, *137*. https://doi.org/10.1016/j.advwatres.2020.103512

EUROSTAT.(2021). *Agricultural production – crops* Retrieved from https://ec.europa.eu/eurostat/en/web/main/data/database. Accessed: 1 June 2021.

FAO Global Statistical Yearbook. (2021). *FAO Regional Statistical Yearbooks*. Retrieved from http://www.fao.org/faostat/en/#data/QC. Accessed: 1 June 2021.

Fischer, E. M., Seneviratne, S. I., Vidale, P. L., Lüthi, D., & Schär, C. (2007). Soil moisture–atmosphere interactions during the 2003 European summer heat wave. *Journal of Climate*, *20*(20), 5081–5099. https://doi.org/10.1175/jcli4288.1

Flach, M., Sippel, S., Gans, F., Bastos, A., Brenning, A., Reichstein, M., & Mahecha, M. D. (2018). Contrasting biosphere responses to hydrometeorological extremes: Revisiting the 2010 western Russian heatwave. *Biogeosciences*, *16*, 6067–6085. https://doi.org/10.5194/bg-15-6067-2018

Frieler, K., Lange, S., Piontek, F., Reyer, C. P. O., Schewe, J., Warszawski, L., & Yamagata, Y. (2017). Assessing the impacts of 1.5 c global warming—Simulation protocol of the inter-sectoral impact model intercomparison project (ISIMIP2b). *Geoscientific Model Development*, *10*(12), 4321–4345. https://doi.org/10.5194/gmd-10-4321-2017

Gudmundsson, L., Bremnes, J. B., Haugen, J. E., & Engen-Skaugen, T. (2012). Downscaling RCM precipitation to the station scale using statistical transformations–a comparison of methods. *Hydrology and Earth System Sciences*, *16*(9), 3383–3390. https://doi.org/10.5194/hess-16-3383-2012

Gupta, H. V., Kling, H., Yilmaz, K. K., & Martinez, G. F. (2009). Decomposition of the mean squared error and NSE performance criteria: Implications for improving hydrological modelling. *Journal of hydrology*, *377*(1–2), 80–91. https://doi.org/10.1016/j.jhydrol.2009.08.003

Hanel, M., Rakovec, O., Markonis, Y., Máca, P., Samaniego, L., Kyselý, J., & Kumar, R. (2018). Revisiting the recent European droughts from a long-term perspective. *Scientific Reports*, *8*(1), 9499. https://doi.org/10.1038/s41598-018-27464-4

Hari, V., Rakovec, O., Markonis, Y., Hanel, M., & Kumar, R. (2020). Increased future occurrences of the exceptional 2018–2019 Central European drought under global warming. *Scientific Reports*, *10*(1), 1–10. https://doi.org/10.1038/s41598-020-68872-9

Hempel, S., Frieler, K., Warszawski, L., Schewe, J., & Piontek, F. (2013). A trend-preserving bias correction - The ISI-MIP approach. *Earth System Dynamics*, *4*(2), 219–236. https://doi.org/10.5194/esd-4-219-2013

Herrera-Estrada, J. E., Satoh, Y., & Sheffield, J. (2017). Spatiotemporal dynamics of global drought. *Geophysical Research Letters*, *44*(5), 2254–2263.

Hofstra, N., Haylock, M., New, M., & Jones, P. D. (2009). Testing E-OBS European high-resolution gridded data set of daily precipitation and surface temperature. *Journal of Geophysical Research: Atmospheres*, *114*(D21). https://doi.org/10.1029/2009jd011799

Ionita, M., Nagavciuc, V., Kumar, R., & Rakovec, O. (2020). On the curious case of the recent decade, mid-spring precipitation deficit in central Europe. *NPJ Climate and Atmospheric Science*, *3*(49), 1–10. https://doi.org/10.1038/s41612-020-00153-8

Kumar, R., Samaniego, L., & Attinger, S. (2013). Implications of distributed hydrologic model parameterization on water fluxes at multiple scales and locations. *Water Resources Research*, *49*(1), 360–379. https://doi.org/10.1029/2012wr012195

Lloyd-Hughes, B. (2012). A spatio-temporal structure-based approach to drought characterisation. *International Journal of Climatology*, *32*(3), 406–418. https://doi.org/10.1002/joc.2280

Lu, J., Carbone, G. J., & Gao, P. (2017). Detrending crop yield data for spatial visualization of drought impacts in the United States, 1895–2014. *Agricultural and Forest Meteorology*, *237–238*, 196–208. https://doi.org/10.1016/j.agrformet.2017.02.001

Masante, D., Barbosa, P., & Magni, D. (2019). European drought observatory. Retrieved from https://edo.jrc.ec.europa.eu/documents/news/EDODroughtNews201908_Europe.pdf. Accessed: 5 May 2021.

Moravec, V., Markonis, Y., Rakovec, O., Kumar, R., & Hanel, M. (2019). A 250-year European drought inventory derived from ensemble hydrologic modeling. *Geophysical Research Letters*, *46*(11), 5909–5917. https://doi.org/10.1029/2019GL082783

Moravec, V., Markonis, Y., Rakovec, O., Svoboda, M., Trnka, M., Kumar, R., & Hanel, M. (2021). Europe under multi-year droughts: How severe was the 2014–2018 drought period? *Environmental Research Letters*, *16*(3), 034062. https://doi.org/10.1088/1748-9326/abe828

Naumann, G., Cammalleri, C., Mentaschi, L., & Feyen, L. (2021). Increased economic drought impacts in Europe with anthropogenic warming. *Nature Climate Change*, *11*, 485–491. https://doi.org/10.1038/s41558-021-01044-3

Oudin, L., Hervieu, F., Michel, C., Perrin, C., Andréassian, V., Anctil, F., & Loumagne, C. (2005). Which potential evapotranspiration input for a lumped rainfall–runoff model?: Part 2—towards a simple and efficient potential evapotranspiration model for rainfall–runoff modelling. *Journal of Hydrology*, *303*(1), 290–306. https://doi.org/10.1016/j.jhydrol.2004.08.026

Peichl, M., Thober, S., Meyer, V., & Samaniego, L. (2018). The effect of soil moisture anomalies on maize yield in Germany. *Natural Hazards and Earth System Sciences*, *18*(3), 889–906. https://doi.org/10.5194/nhess-18-889-2018

Peters, W., Bastos, A., Ciais, P., & Vermeulen, A. (2020). A historical, geographical and ecological perspective on the 2018 European summer drought. *Philosophical transactions of the royal society B*, *375*(1810), 20190505. https://doi.org/10.1098/rstb.2019.0505

Samaniego, L., Kaluza, M., Kumar, R., Rakovec, O., Schüler, L., Schweppe, R., et al. (2019). Mesoscale Hydrologic Model (v5.10). [Computer software]. Zenodo. https://doi.org/10.5281/ZENODO.3239055

Samaniego, L., Kumar, R., & Attinger, S. (2010). Multiscale parameter regionalization of a grid-based hydrologic model at the mesoscale. *Water Resources Research*, *46*(W05523). https://doi.org/10.1029/2008wr007327

Samaniego, L., Kumar, R., Thober, S., Rakovec, O., Zink, M., Wanders, N., & Attinger, S. (2017). Toward seamless hydrologic predictions across spatial scales. *Hydrology and Earth System Sciences*, *21*(9), 4323–4346. https://doi.org/10.5194/hess-21-4323-2017

Samaniego, L., Kumar, R., & Zink, M. (2013). Implications of parameter uncertainty on soil moisture drought analysis in Germany. *Journal of Hydrometeorology*, *14*(1), 47–68. https://doi.org/10.1175/jhm-d-12-075.1

Samaniego, L., Kumar, R., Zink, M., Mai, J., Boeing, F., Shrestha, P.-K., et al. (2022). *The Soil Moisture Index - SMI program (Version 2.0.5)* [Computer software]. Zenodo. https://doi.org/10.5281/ZENODO.5842486

Samaniego, L., Thober, S., Kumar, R., Wanders, N., Rakovec, O., Pan, M., & Marx, A. (2018). Anthropogenic warming exacerbates European soil moisture droughts. *Nature Climate Change*, *8*(5), 421. https://doi.org/10.1038/s41558-018-0138-5

Samaniego, L., Thober, S., Wanders, N., Pan, M., Rakovec, O., Sheffield, J., & Kumar, R. (2019). Hydrological forecasts and projections for improved decision-making in the water sector in Europe. *Bulletin of the American Meteorological Society*, *100*(12), 2451–2471. https://doi.org/10.1175/bams-d-17-0274.1

Scheff, J., & Frierson, D. M. (2014). Scaling potential evapotranspiration with greenhouse warming. *Journal of Climate*, *27*(4), 1539–1558. https://doi.org/10.1175/jcli-d-13-00233.1

Seneviratne, S. I., Corti, T., Davin, E. L., Hirschi, M., Jaeger, E. B., Lehner, I., & Teuling, A. J. (2010). Investigating soil moisture–climate interactions in a changing climate: A review. *Earth-Science Reviews*, *99*(3–4), 125–161. https://doi.org/10.1016/j.earscirev.2010.02.004

Sheffield, J., Goteti, G., Wen, F., & Wood, E. F. (2004). A simulated soil moisture based drought analysis for the United States. *Journal of Geophysical Research: Atmospheres*, *109*(D24). https://doi.org/10.1029/2004jd005182

Stanke, C., Kerac, M., Prudhomme, C., Medlock, J., & Murray, V. (2013). Health effects of drought: A systematic review of the evidence. *PLoS Currents*, *5*. https://doi.org/10.1371/currents.dis.7a2cee9e980f91ad7697b570bcc4b004

Tolson, B. A., & Shoemaker, C. A. (2007). Dynamically dimensioned search algorithm for computationally efficient watershed model calibration. *Water Resources Research*, *43*(1). https://doi.org/10.1029/2005WR004723

Trnka, M., Feng, S., Semenov, M. A., Olesen, J. E., Kersebaum, K. C., Rötter, R. P., et al. (2019). Mitigation efforts will not fully alleviate the increase in water scarcity occurrence probability in wheat-producing areas. *Science Advances*, *5*(9), eaau2406. https://doi.org/10.1126/sciadv.aau2406

Van Lanen, H. A., Laaha, G., Kingston, D. G., Gauster, T., Ionita, M., Vidal, J.-P., et al. (2016). Hydrology needed to manage droughts: The 2015 European case. *Hydrological Processes*, *30*(17), 3097–3104. https://doi.org/10.1002/hyp.10838

Vidal, J.-P., Martin, E., Franchistéguy, L., Habets, F., Soubeyroux, J.-M., Blanchard, M., & Baillon, M. (2010). Multilevel and multiscale drought reanalysis over France with the Safran-Isba-Modcou hydrometeorological suite. *Hydrology and Earth System Sciences*, *14*(3), 459–478. https://doi.org/10.5194/hess-14-459-2010

Vogel, M. M., Zscheischler, J., Wartenburger, R., Dee, D., & Seneviratne, S. I. (2019). Concurrent 2018 hot extremes across Northern Hemisphere due to human-induced climate change. *Earth's Future*, *7*(7), 692–703. https://doi.org/10.1029/2019ef001189

Warszawski, L., Frieler, K., Huber, V., Piontek, F., Serdeczny, O., & Schewe, J. (2014). The inter-sectoral impact model intercomparison project (ISI–MIP): Project framework. *Proceedings of the National Academy of Sciences*, *111*(9), 3228–3232. https://doi.org/10.1073/pnas.1312330110

Williams, A. P., Cook, E. R., Smerdon, J. E., Cook, B. I., Abatzoglou, J. T., Bolles, K., & Livneh, B. (2020). Large contribution from anthropogenic warming to an emerging North American megadrought. *Science*, *368*(6488), 314–318. https://doi.org/10.1126/science.aaz9600

Zhou, H., Liu, Y., & Liu, Y. (2019). An approach to tracking meteorological drought migration. *Water Resources Research*, *55*(4), 3266–3284. https://doi.org/10.1029/2018wr023311

Zink, M., Samaniego, L., Kumar, R., Thober, S., Mai, J., Schäfer, D., & Marx, A. (2016). The German drought monitor. *Environmental Research Letters*, *11*(7), 074002. https://doi.org/10.1088/1748-9326/11/7/074002